

SURFACE WAVE LOSSES AT DISCONTINUITIES
IN MILLIMETER WAVE INTEGRATED
TRANSMISSION LINES

R. W. Jackson and D. M. Pozar

Department of Electrical and Computer Engineering
University of Massachusetts
Amherst, MA 01003

ABSTRACT

Using a fullwave analysis we have calculated the loss due to surface wave and space wave radiation at three types of discontinuities in planar millimeter wave transmission lines. The open ended microstrip, the microstrip gap and the short circuited coplanar waveguide were investigated on electrically thick substrates. Results on typical high dielectric substrates are presented.

Introduction

Currently, the analyses of discontinuities in planar waveguiding structures do not consider effects which are likely to be important at high frequencies on electrically thick substrates (i.e., millimeter wave monolithic circuits). Microstrip discontinuities such as the open end or gap are usually modeled using the quasistatic method developed by Gopinath [1] and others. This method gives satisfactory results on electrically thin substrates but will be less accurate at higher frequencies where surface wave and space wave radiation becomes significant. A more accurate routine has been developed by Koster and Jansen [2] using fully electromagnetic solutions. The configurations analyzed by Jansen are enclosed in perfectly conducting boxes and thus also do not include surface waves or other parasitic waves. We have analyzed three discontinuities: the microstrip open end, the microstrip gap and the coplanar waveguide short circuit. In each case a rigorous integral equation was formulated using the appropriate grounded dielectric slab Green's function. This equation was then solved numerically. Radiation and surface wave losses are included. We describe the method for the representative case of an open ended microstrip, then describe the modification for the analysis of a microstrip gap and of a coplanar waveguide short. Finally, results are presented.

Formulation for the Microstrip Open End

We analyze herein a perfectly conducting microstripline of width W on a grounded dielectric slab of thickness, d (see figure 1). The microstrip extends from minus infinity to $x=0$. To

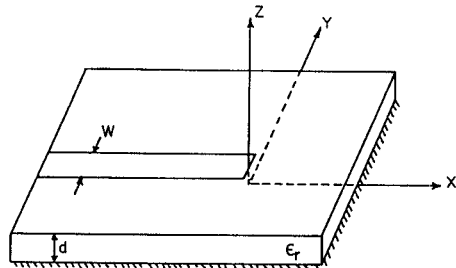


Figure 1. Open Ended Microstrip

derive the integral equation we start with the expression for the x directed electric field on the dielectric/air interface due to an arbitrary x -directed surface current, J_x , also on the dielectric/air interface,

$$E_x(x, y, d) = \left\{ \int_{-\infty}^{\infty} \int_{-\infty}^{\infty} G(x, y, x_o, y_o) J_x(x_o, y_o, d) dx_o dy_o \right\} \quad (1)$$

where $G(x, y, x_o, y_o)$ is the grounded dielectric slab Green's function given in the appendix. The fields generated by equation (1) satisfy all boundary conditions at the dielectric interface and at the ground plane. Surface waves are included exactly and come about as a result of the poles in the Fourier transforms of the Green's function. An integral equation results when J_x is constrained such that E_x is zero on the perfectly conducting microstrip. We then split the current into a known impressed current J_x^i and an unknown excited current

J_x^e resulting in

$$\left\{ \int_{-\infty}^{\infty} \int_{-\infty}^{\infty} G(x, y, x_o, y_o) [J_x^e(x_o, y_o, d) + J_x^i(x_o, y_o, d)] dx_o dy_o \right\} = 0 \quad \text{for } |y| < W/2, z < 0 \quad (2)$$

We solve this equation numerically by expanding J_x^e into a sum of N known functions multiplied

by unknown constants and then forming N constraining equations by taking weighted averages over all x, y space. The expansion modes include two finite length sinusoids in quadrature with respect to each other as well as several short piecewise sinusoids located in the vicinity of the open end. The finite length sinusoids (reflected wave) were an approximation to an infinite exponential wavetrain. Three or four periods were found to form a sufficiently good approximation. The wavelengths were chosen to be equal to the corresponding infinite microstrip mode. The impressed (incident) current was also made up of two finite length sinusoids in quadrature. The weighting functions were all piecewise sinusoids. All weighting and expansion functions were, initially, uniform in the transverse direction. Finally one solves the resulting matrix equation for the amplitude of the reflected wave.

Microstrip Gap

The microstrip gap discontinuity is shown in figure 2. In order to modify our open end program to analyze the gap we add another pair of finite length quadrature sinusoids to our excited current, J_x^e . These new modes exist only for $x > G$ and represent the transmitted wave. Three or four piecewise sinusoidal modes are also added for $x > G$ near the

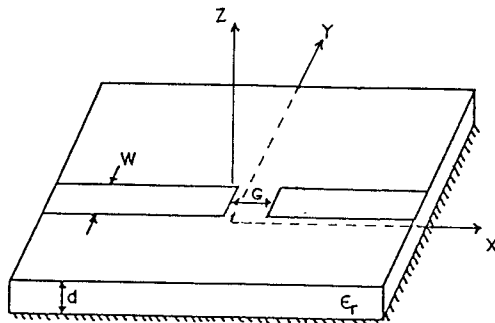


Figure 2. Microstrip Gap Discontinuity

gap. A matrix equation for the mode amplitudes is formed. We then solve for the reflected and transmitted wave amplitudes (S_{11}, S_{21}).

Coplanar Waveguide Short Circuit

Coplanar waveguide has been considered as a millimeter wave transmission medium due to the fact that it may have advantages in size, dispersion and grounding of active devices. It may also be less susceptible to surface wave generation when compared with microstrip at millimeter wave frequencies. In view of this last possibility we are investigating the surface wave generation characteristics of a shorted coplanar waveguide. To do this we merely replace the Green's function in equation 2 with a new Green's function and replace the currents, J_x^i and J_x^e with coplanar waveguide slot fields [3] E_y^i and E_y^e . The new Green's function relates the slot field in the

ground plane of a dielectric slab to the difference between the tangential magnetic field just above the ground plane and the tangential magnetic field just below or, equivalently, to the surface current on the ground plane.

$$J_y(x, y, o) = \int_{-\infty}^{\infty} \int_{-\infty}^{\infty} G^S(x, y, x_o, y_o) E_y(x_o, y_o, o) dx_o dy_o \quad (3)$$

E_y is now constrained such that J_y is zero wherever a slot exists (see reference [3]). The remaining analysis is similar to the microstrip open end.

Results

In this section we present our results for the open ended microstrip the microstrip gap, and the short circuited coplanar waveguide.

Our open end results agree well with data previously published (measured and computed) on low dielectric substrates. We have calculated the end conductance on $\epsilon_r = 2.32$ dielectric and compared it with the measured and computed results of James and Henderson [4]. Very close agreement occurs for thin dielectrics. Length extensions (phase) were also computed but were found to be much more sensitive to current distribution with respect to the transverse coordinate. Instead of uniform distribution, we found that a distribution which enforced the edge condition,

$$J_x(x, y) = \frac{f(x)}{\sqrt{1-(2y/w)^2}},$$

gave length extensions that, for then $\epsilon_r = 12.8$ substrates, agreed with quasi-static results when w/d is less than 2. Figure 3 shows representative new results on an $\epsilon_r = 12.8$ substrate. Reflection coefficient magnitude vs. frequency (electrical thickness) is plotted. Note that quasistatic analysis or analysis in a perfectly conducting box would not give this result.

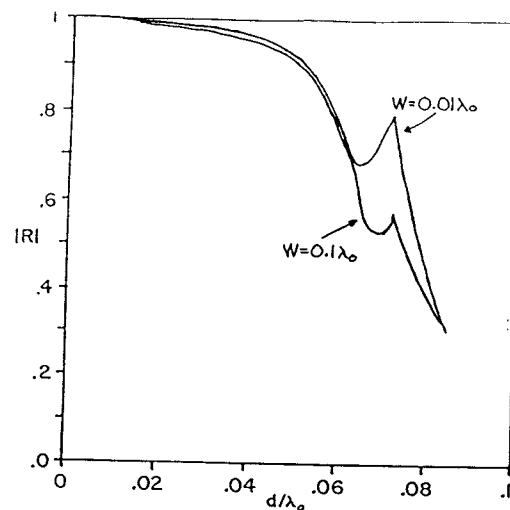


Figure 3. Magnitude of Reflection Coefficient from Microstrip Open Ended on $\epsilon_r = 12.8$ dielectric.

Scattering parameters were computed for the microstrip gap discontinuity on low and high dielectric constant substrates. On electrically thin substrates these results agreed very favorably with quasistatic results. Differences occurred for thicker substrates. In Figure 4 we plot a measure of loss vs. frequency for a particular gap on $\epsilon_r = 12.8$ substrate. Notice that the loss to radiation and surface waves increases to a maximum and then decreases. This drop off is explained by remembering that a gap discontinuity is modeled by a series capacitor. At high frequencies this capacitor looks like a series short circuit and thus like no discontinuity at all.

In figure 5 we plot reflection coefficient magnitude vs. d/λ_0 (frequency) for a short circuited coplanar waveguide on an $\epsilon_r = 12.8$ substrate.

We note that in this case losses are due to radiation from the top and bottom of the ground plane and surface waves. As one would expect, these losses are small due to the close proximity of two oppositely polarized fields.

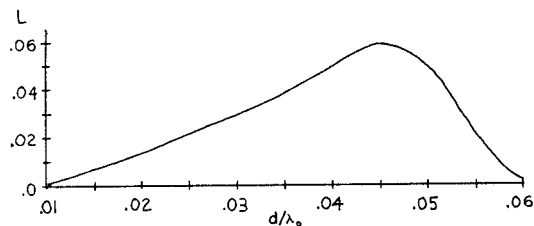


Figure 4. Measure of Loss for a Microstrip Gap Discontinuity. $L = 1 - |S_{11}|^2 - |S_{21}|^2$, $\epsilon_r = 12.8$, $G = .2d$, $W = 2.5d$

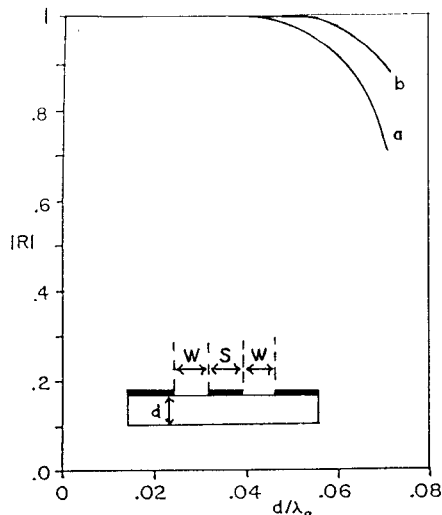


Figure 5. Magnitude of Reflection Coefficient from a Coplanar Waveguide Short on $\epsilon_r = 12.8$ Substrate. (a) $W/d = 1.$, $S/d = 1.4$.
(b) $W/d = .5$, $S/d = .7$

Conclusion

A technique for the full wave analysis of the microstrip open circuit, the microstrip gap and the coplanar waveguide short circuit are presented. Losses to surface waves and radiation are important effects which are included. Computed results on $\epsilon_r = 12.8$ substrates are presented for the microstrip open end, microstrip gap, and coplanar waveguide short.

Acknowledgement: This work was supported by RADC (Hanscom), U.S. Air Force, under contract F19628-84-K-0022 and by the Air Force Office of Scientific/AFSC, United States Air Force, under Contract F49620-82-C-0035.

References

- [1] "Capacitance Parameters of Discontinuities in Microstripline", A. Gopinath and C. Gupta, IEEE Microwave Theory and Techniques, MTT-25, Oct. 1977, pp. 819-822.
- [2] "The Equivalent Circuit of the Asymmetrical Series Gap in Microstrip and Suspended Substrate Lines", N.H.L. Koster and R.H. Jansen, IEEE Microwave Theory and Techniques, MTT-30, August 1982.
- [3] "Analysis of Coupled Slots and Coplanar Strips on Dielectric Substrate", J.B. Knorr and K. Kuchler, IEEE Microwave Theory and Techniques, MTT-23, #7, July 1975.
- [4] "High Frequency Behavior of Microstrip Open Circuit Terminations", J.R. James and A. Henderson, IEEE J. Microwave Optics and Acoustics, Vol. 3, pp. 205-211, 1979.

Appendix

The grounded dielectric slab Green's function is,

$$G(x, y, x_0, y_0) = \frac{-jZ_0}{4\pi^2 k_0} \left\{ \int_{-\infty}^{\infty} \int_{-\infty}^{\infty} Q(k_x, k_y) \cdot e^{jk_x(x-x_0)} e^{jk_y(y-y_0)} dk_x dk_y, \right.$$

where

$$Q(k_x, k_y) = \frac{(\epsilon_r k_0^2 - k_x^2) k_2 \cos k_1 d + j k_1 (k_0^2 - k_x^2) \sin k_1 d}{T_e T_m}$$

$\sin k_1 d$,

$$T_e = k_1 \cos k_1 d + j k_2 \sin k_1 d,$$

$$T_m = \epsilon_r k_2 \cos k_1 d + j k_1 \sin k_1 d,$$

$$k_1^2 = \epsilon_r k_0^2 - \beta^2, \quad (Im k_1 < 0)$$

$$k_2^2 = k_0^2 - \beta^2, \quad (Im k_2 < 0)$$

$$\beta^2 = k_x^2 + k_y^2,$$

$$Z_0 = \sqrt{\mu_0 / \epsilon_0} \quad .$$